Myriocin slows the progression of established atherosclerotic lesions in apolipoprotein E gene knockout mice[S]

Elias N. Glaros,* Woojin S. Kim,* Carmel M. Quinn,† Wendy Jessup,† Kerry-Anne Rye,§ and Brett Garner[1],*,**

Prince of Wales Medical Research Institute,* Randwick NSW 2031, Australia; Centre for Vascular Research,† University of New South Wales, Sydney NSW 2052, Australia; Heart Research Institute,§ Sydney NSW 2050, Australia; and School of Medical Sciences,** University of New South Wales, Sydney NSW 2052, Australia

Abstract The serine palmitoyl transferase inhibitor myriocin potently suppresses the development of atherosclerosis in apolipoprotein E (apoE) gene knockout (apoE$^{-/-}$) mice fed a high-fat diet. This is associated with reduced plasma sphingomyelin (SM) and glycosphingolipid levels. Furthermore, oral administration of myriocin decreases plasma cholesterol and triglyceride (TG) levels. Here, we aimed to determine whether myriocin could inhibit the progression (or stimulate the regression) of established atherosclerotic lesions and to examine potential changes in hepatic and plasma lipid concentrations. Adult apoE$^{-/-}$ mice were fed a high-fat diet for 30 days, and lesion formation was histologically confirmed. Replicate groups of mice were then transferred to either regular chow or chow containing myriocin (0.3 mg/kg/day) and maintained for a further 60 days. Myriocin significantly inhibited the progression of established atherosclerosis when combined lesion areas (aortic sinus, arch, and celiac branch point) were measured. Although the inhibition of lesion progression was observed mainly in the distal regions of the aorta, regression of lesion size was not detected. The inhibition of lesion progression was associated with reductions in hepatic and plasma SM, cholesterol, and TG levels and increased hepatic and plasma apoA-I levels, indicating that the modulation of pathways associated with several classes of atherogenic lipids may be involved.—Glaros, E. N., W. S. Kim, C. M. Quinn, W. Jessup, K-A. Rye, and B. Garner. **Myriocin slows the progression of established atherosclerotic lesions in apolipoprotein E gene knockout mice. *J. Lipid Res.* 2008.** 49: **324–331.**

Supplementary key words atherosclerosis • sphingomyelin • glycosphingolipids • sphingolipid synthesis inhibition

Atherosclerosis is a major cause of cardiovascular disease and accounts for ~50% of all deaths in Westernized countries (1). Atherosclerosis develops as a consequence of multiple pathways that involve inflammation, dysregulated cellular proliferation, and lipid accumulation (2, 3). It is established that 3-hydroxy-3-methylglutaryl-CoA reductase inhibitors (statins) reduce plasma cholesterol levels and that this is clearly associated with reduced cardiovascular events and the stabilization of vulnerable plaques (4, 5). However, pharmacologic approaches to stimulate the regression of atherosclerotic lesions (rather than halting progression) remain an area of intense investigation. There is evidence that very high-intensity statin therapy may indeed stimulate the regression of atherosclerosis in humans; however, this area is controversial, and very high statin doses may not be tolerated well by all patients (6, 7). Thus, the search for novel antiatherosclerotic therapies that could induce lesion regression continues.

In addition to cholesterol, the accumulation of sphingomyelin (SM) and glycosphingolipids (GSLs) in atherosclerotic lesions is well known (8–10). Similar to cholesterol, plasma SM and GSL levels are also correlated with atherosclerosis risk (11–13). There is also evidence for proatherogenic effects of both SM and GSLs. For example, LDL extracted from human atherosclerotic lesions is highly enriched with SM compared with plasma LDL (14), and SM carried into the arterial wall (associated with LDL) is acted upon by sphingomyelinase, increasing lesion ceramide levels and promoting LDL aggregation (15). In the case of GSLs, several proatherogenic properties have been proposed. These include the findings that lactosylceramide promotes cholesterol accumulation in macrophage foam cells (16), inhibits cellular cholesterol removal via the ABCA1/apolipoprotein A-I (apoA-I) pathway (17), induces monocyte adhesion to endothelial cells (18), and stimulates

Manuscript received 6 June 2007 and in revised form 19 September 2007 and in re-revised form 30 October 2007.

Published, JLR Papers in Press, October 31, 2007.
DOI 10.1194/jlr.M700261-JLR200

Abbreviations: apoE, apolipoprotein E; GSL, glycosphingolipid; HF, high-fat chow; SM, sphingomyelin; TG, triglyceride.

[1] To whom correspondence should be addressed.
e-mail: brett.garner@unsw.edu.au

[S] The online version of this article (available at http://www.jlr.org) contains supplementary data.

vascular smooth muscle cell proliferation (19). Other studies have reported that ganglioside GM3 accelerates LDL uptake by macrophages, which results in the generation of lipid-laden foam cells (20). In more general terms, the vascular accumulation of GSLs could affect atherogenesis via the regulation of cellular signaling, activation, recognition, differentiation, fibrinolytic activity, nitric oxide production, and response to growth factors (13, 21).

The potential for sphingolipid synthesis inhibitors to prevent atherosclerosis recently received attention (13, 22), and data from our group and others indicate that the serine palmitoyl transferase inhibitor myriocin dramatically reduces the development of atherosclerotic lesions in apoE gene knockout (apoE$^{-/-}$) mice (23–25). Moreover, myriocin administered by intraperitoneal injection reduces plasma SM and GSL levels without affecting cholesterol levels, and this results in dramatic inhibition of atherosclerotic lesion size (ranging from ~40% to 70% inhibition depending on the aortic site assessed) (24, 25). In studies by Park et al. (23), reductions in lesion area were even more impressive, with a 93% reduction in lesion area observed when mice received myriocin orally (a dose of 0.3 mg/kg body weight per day, mixed in the diet), although in this case oral myriocin reduced plasma cholesterol levels by 41%, thereby potentially confounding the specific antiatherogenic effects associated with reducing plasma SM and GSL levels. Although these studies examined the impact of myriocin during disease development, the potential for this compound to retard the progression of (or promote the regression of) preexisting atherosclerotic lesions has not been examined. In the present study, we addressed this important issue and show that with a 60 day 0.3 mg/kg/day oral treatment regime, myriocin significantly inhibits the progression of preexisting lesions but does not promote lesion regression.

MATERIALS AND METHODS

Materials

All organic solvents were of analytical grade and purchased from Merck (Darmstadt, Germany). Purified leech (*Macrobdella decora*) ceramide glycanase (EC 3.2.1.123) was from V-Labs (Covington, LA) and myriocin was from Sigma (Castle Hill, Australia). All other reagents were of the highest purity available and purchased through standard commercial suppliers.

Animals and diet

Male apoE$^{-/-}$ mice were supplied by the Animal Resources Centre (Canning Vale, Australia). From 8 weeks of age, three groups of 10 mice were fed high-fat chow [HF; 22% (w/w) fat, 0.15% (w/w) cholesterol] (Diet No. SF00-219; Specialty Feeds, Glen Forest, Australia) for 30 days. A control group was culled to establish lesion severity, and the remaining two groups were continued for 60 days on a standard chow (Diet No. SF06-055; Specialty Feeds) or standard chow containing 2.2 mg/kg myriocin. The concentration of myriocin in the diet was calculated on the assumption that the mice would consume an average of 6 g of chow per day, resulting in a myriocin dose of 0.3 mg/kg/day (23). This study was approved by the University of New South Wales Animal Care and Ethics Committee (approval No. ACEC05/39A) and conforms with the U.S. Public Health Service Policy on the Humane Care and Use of Laboratory Animals.

Assessment of atherosclerotic lesions

All mice were fasted overnight. Plasma was collected and perfusion-fixed hearts and aortas were dissected, and the sinus, arch, and abdominal (at the celiac branch point) aortic sections were prepared for the assessment of lesion area as described previously (25). Morphometric data were collected for the three sites after sections were subjected to Verhoeff staining. The data from the different aortic sites were used to provide site-specific aortic lesion data and, after pooling for each individual mouse, to give average values for aortic lesion severity (see the supplementary data for additional details).

Analysis of plasma lipids and glucose

Plasma triglyceride (TG), phosphatidylcholine, and SM analysis was achieved by enzymatic methods described previously (13, 25, 26). Plasma cholesterol was analyzed using a commercially available kit according to the manufacturer's instructions (Amplex Red Cholesterol Assay Kit; Invitrogen, Mount Waverley, Australia). Plasma GSL analysis was achieved by normal-phase HPLC (13, 25) with minor modifications. In the present study, 0.1 unit of ceramide glycanase was used to hydrolyze total neutral and charged GSLs in 40 μl of plasma, and the resultant GSL-derived glycans were fluorescently labeled with 2-aminobenzamide and analyzed as a single sample (rather than analyzing neutral and charged glycans separately). Plasma glucose concentration was analyzed using a commercially available kit according to the manufacturer's instructions (Infinity Glucose Reagent; Thermo Scientific, Noble Park, Australia).

Quantitative real-time PCR analysis of hepatic apoB, apoA-I, and ABCA1 mRNA

Mice were euthanized and the liver was dissected free of contaminating tissues; half was placed immediately in RNALater (Ambion) for mRNA analysis, and the other half was snap-frozen for protein and lipid analysis (see below). RNA was isolated from the tissue using TRIzol reagent (Invitrogen) according to the manufacturer's protocol. All procedures were carried out using RNase-free reagents. RNA was reverse-transcribed into cDNA using Moloney murine leukemia virus reverse transcriptase and random primers (Promega). cDNA generated from the reverse transcription of total RNA was used as a template in the quantitative real-time PCR assay. Quantitative real-time PCR amplification was carried out using a Mastercycler ep realplex S (Eppendorf) and the fluorescent dye SYBR Green (Eppendorf) according to the manufacturer's protocol. Briefly, each reaction (20 μl) contained 20 pmol of primers, 1× Real MasterMix, 1× SYBR Green, and 1 μl of template. Amplification was carried out with 40 cycles of denaturation (94°C, 30 s), annealing (57°C, 30 s), and extension (72°C, 30 s). All gene expression was normalized to GAPDH. The primer sequences (5′–3′) and PCR product sizes are as follows. ABCA1 (106 bp) forward, GCTCTGGGAGAGGATGCTGA, and reverse, CGTTTCCGGGAAGTGTCCTA; apoA-I (129 bp) forward, GGCACGTATGGCAGCAAGAT, and reverse, CCAAGGAGGAGGATTCAAACTG; apoB (142 bp) forward, TTGGCAAACTGCATAGCATCC, and reverse, TCAAATTGGGACTCTCCTTTAGC; GAPDH (83 bp) forward, TGGTGAAGCAGGCATCTGAG, and reverse, TGCTGTTGAAGTCGCAGGAG.

Western blot analysis of liver and plasma apoA-I

Liver samples (50 mg) were homogenized in 1.5 ml Eppendorf tubes using Pellet Pestles (catalog No. Z359947; Sigma-Aldrich)

in 1 ml of RIPA buffer [20 mM Tris-HCl, pH 7.5, 150 mM NaCl, 1 mM EDTA, 1% Nonidet P-40, 0.5% deoxycholate, 0.1% SDS, and protease inhibitors (catalog No. 11836153001; Roche)]. Homogenates were diluted 1:10 in Milli-Q water (3.5 μl in 35 μl total) and mixed with 7 μl of 5× Laemmli sample buffer (total volume, 42 μl). Plasma samples were similarly diluted 1:10 with Milli-Q water and mixed with 7 μl of 5× Laemmli sample buffer. All samples were heated at 95°C for 5 min and briefly centrifuged. Samples (10 μl) were run on 12% SDS-PAGE gels using a Bio-Rad mini gel system. The proteins were transferred to 0.45 μm Trans-Blot nitrocellulose membranes (catalog No. 162-0115; Bio-Rad), and the membranes were probed with 1:1,000-diluted rabbit anti-human apoA-I polyclonal antibody that cross-reacts strongly with mouse apoA-I (catalog No. 178422; Calbiochem) and detected with 1:750-diluted HRP-conjugated anti-rabbit secondary antibody (catalog No. 2012-09; DAKO) and ECL advanced detection reagents (GE Healthcare). The intensity of the apoA-I bands was measured using ImageJ software, which is available in the public domain (http://rsb.info.nih.gov/ij/).

Liver lipid analysis

Liver samples (200 mg) were homogenized in 1 ml of methanol using a Pellet Pestle (Sigma-Aldrich). Samples were transferred to a glass extraction tube and 5 ml of hexane was added. Samples were vortexed and centrifuged at 1,000 *g* for 5 min. The hexane phase was removed to a clean glass tube and evaporated to dryness under vacuum. The process was repeated with a second 5 ml of hexane, which was added to the residue of the first extraction and again dried under vacuum. The residue was resuspended in 200 μl of isopropanol, and 10 μl was analyzed by reversed-phase HPLC using a Supelcosil LC 18 column and UV absorbance detection at a wavelength of 120 nm. HPLC solvent conditions were as follows: mobile phase composition, isopropanol-acetonitrile-water (54:44:2, v/v/v); flow rate, 1 ml/min; total run time, 140 min. HPLC profiles were quantified for cholesterol, TG, and cholesteryl ester fractions as described previously (27, 28). Liver SM was analyzed by removing 50 μl of the 1 ml methanol phase remaining after the two 5 ml hexane extractions described above. The 50 μl sample was dried at 22°C under a stream of nitrogen gas, and the residue was analyzed for SM using the enzymatic method described previously (25, 26).

Statistical analysis

All data are presented as means ± SEM. Statistical significance for differences in lesion areas and plasma lipid concentrations was determined using the Mann-Whitney U test and Student's *t*-test, respectively. Differences were considered significant at $P < 0.05$.

RESULTS

To assess the potential for myriocin to inhibit the progression of established atherosclerosis, adult male apoE$^{-/-}$ mice were fed a HF diet for 30 days to induce aortic lesions. Assessment of the aorta at the sinus, arch, and celiac branch point confirmed that lesions were clearly detectable at all sites in the first group of 10 mice (**Fig. 1**). Significant lesions were present at the aortic sinus and the inner curvature of the aortic arch and at the proximal branch points of the arch as well as in the abdominal aorta at the celiac branch (Fig. 1). Although atherosclerotic lesions were clearly detectable in the mice fed a HF diet for 30 days (Fig. 1), they were not as complex or extensive as those seen after long-term HF feeding and are therefore referred to here as "established" atherosclerotic lesions. The moderate extent of lesion development at this time point is consistent with previous data (29). By contrast, long-term feeding with a HF diet (i.e., >6 months) produces advanced lesions in apoE$^{-/-}$ mice that are calcified and contain an extensive lipid-rich necrotic core and frequent intraplaque hemorrhages (30). Fasted plasma and liver samples were collected and stored at −80°C for future lipid analysis at the same time that the first group (group I) of mice were euthanized for baseline lesion assessment.

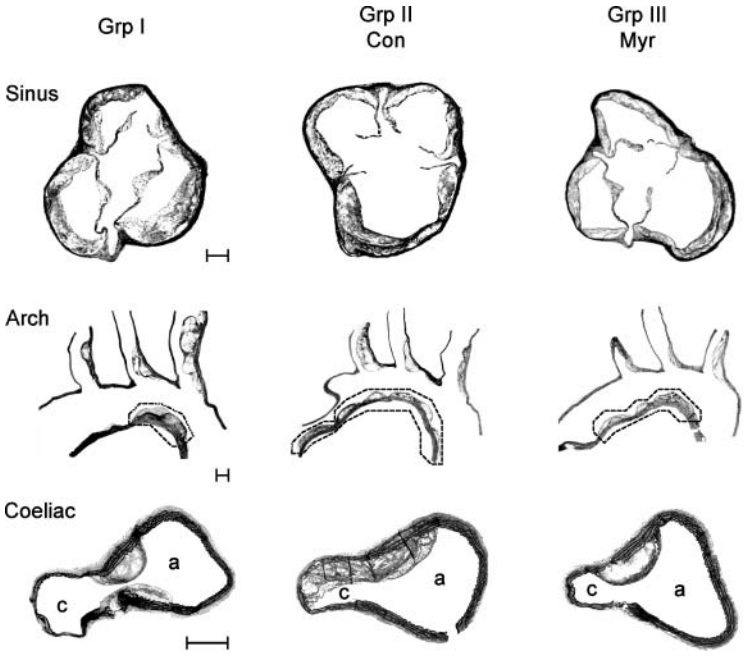

Fig. 1. Histological assessment of atherosclerosis at the aortic sinus, arch, and celiac branch point. Apolipoprotein E gene knockout (apoE$^{-/-}$) mice were fed a high-fat diet for 30 days (Grp I) and then switched to regular chow (Grp II) or regular chow containing myriocin (0–3 mg/kg/day) (Grp III) for a further 60 days. Lesions were assessed at the aortic sinus, arch, and celiac branch point. The lumen of the abdominal aorta (a) and celiac artery (c) are marked at the celiac branch. The dashed lines indicate the region of the arch that was assessed for lesion area. Representative sections are shown after Verhoeff staining. Bars = 250 μm.

After 30 days of the HF diet, the remaining two groups of 10 mice were switched to either regular chow or regular chow plus myriocin for a further 60 days. After both groups were euthanized, fasted plasma and liver tissues were collected and aortas were removed and assessed for atherosclerotic lesion development (Fig. 1). Mice were also weighed at the start of the study and at the time of death. All three groups of mice gained weight during the study (**Fig. 2**). A significant weight gain was also detected when the mice fed the HF diet for 30 days (group I) were compared with mice receiving regular chow (group II) or regular chow plus myriocin (group III) (Fig. 2). The average weight of mice receiving myriocin (group III) was 4.9% lower than that of control mice (group II) at the time of death (30.41 ± 0.56 g vs. 31.96 ± 0.29 g; $P = 0.031$), indicating that oral myriocin treatment had a minor impact on weight gain. This is consistent with previous reports indicating that myriocin is well tolerated by apoE$^{-/-}$ mice (23–25, 31).

Fasted plasma lipid and glucose data for all three groups of mice are presented in **Table 1**. The mice that were switched from the HF diet to regular chow for 60 days exhibited a significant 15% decrease in plasma cholesterol and a significant 58% increase in plasma phosphatidylcholine. No significant changes in TG, SM, GSL, or glucose levels were detected between group I and group II mice (Table 1). The presence of myriocin in the diet dramatically altered the plasma lipid profile. Most notably, compared with the mice switched to regular chow alone, the myriocin-treated group showed significant decreases in cholesterol, TG, SM, and GSL concentrations (57, 18, 54, and 21%, respectively). In the case of cholesterol and SM, the myriocin-treated group also exhibited lower levels than measured in the "baseline" group of mice euthanized directly after 30 days on the HF diet. The reductions in cholesterol, TG, and SM induced by myriocin in the regular chow diet are in general agreement with previous data demonstrating reductions in these lipids when myriocin was given as a component of a HF diet (23, 31). The demonstration that oral delivery of myriocin also significantly reduced plasma GSL levels confirms and extends our recent work showing that intraperitoneally administered myriocin reduces plasma GSL levels in apoE$^{-/-}$ mice fed a HF diet (25).

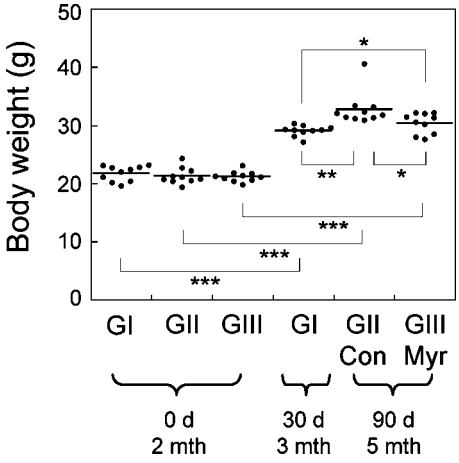

Fig. 2. Total body weight of mice. ApoE$^{-/-}$ mice were fed a high-fat diet for 30 days (GI) and then switched to regular chow (GII) or regular chow containing myriocin (0–3 mg/kg/day) (GIII) for a further 60 days. Body weight was measured at 0 days (0 d) when all mice were 2 months old and at the time of death, 30 days (30 d) for GI and 90 days (90 d) for GII and GIII. * $P < 0.05$, ** $P < 0.01$, *** $P < 0.0001$, assessed by Student's *t*-test.

The primary aim of this study was to examine whether myriocin could affect the further development of established atherosclerotic lesions. When overall lesion severity was assessed by combining the morphometric data derived from the three aortic sites in each mouse (see Materials and Methods), there was a significant advancement of lesion severity when mice with established lesions were fed regular chow for a further 60 days (**Fig. 3A**). Myriocin treatment did not completely halt the progression of atherosclerosis over this time; however, the increase in relative lesion area observed in mice fed regular chow for 60 days was inhibited by 60% with oral myriocin treatment (Fig. 3A). The site-specific action of myriocin was also examined in the mice fed regular chow for 60 days compared with the myriocin-treated group, and it was clear that the greatest effects of the drug were observed in the abdominal aorta (Fig. 3B). When the data for the arch and sinus were analyzed alone, a nonsignificant trend for reduced lesion severity with myriocin treatment was observed (Fig. 3B). This analysis indicates that the significant inhibition of lesion progression observed overall (Fig. 3A) was primarily influenced by the inhibition of atherosclerosis in the abdominal aorta. The propensity for myriocin action to be more pronounced at the distal aortic sites is also consistent with our previous data showing that intraperitoneal administration of myriocin predominantly inhibits atherosclerosis in the abdominal aorta (25).

Previous data indicate that myriocin (0–3 mg/kg/day administered as diet admix) reduces hepatic SM levels by ~50% and also (0–3 mg/kg/day administered by oral gavage for 5 days) induces hepatic apoA-I mRNA expression in apoE$^{-/-}$ mice (23, 31). To examine whether similar changes occurred in the liver under our present experimental conditions, we investigated the impact of myriocin treatment on liver SM as well as the major hepatic storage lipids cholesterol and TG. In addition, hepatic apoA-I expression at both the mRNA and protein levels was also assessed. Myriocin treatment (group III compared with group II) reduced hepatic SM concentration by 39% (**Fig. 4**), confirming that the potent serine palmitoyl transferase inhibitor was active in vivo. In addition, statistically significant reductions in hepatic cholesterol (10%) and TG (30%) concentrations were also observed in the myriocin-treated mice compared with the control animals (group III versus group II) (Fig. 4). The cholesteryl ester fraction accounted for a minor proportion of total liver cholesterol and was also reduced significantly with myriocin treatment (Fig. 4). These data indicate that myriocin modulates hepatic lipid homeostasis and suggest that this is likely to make an important contribution to the antiatherogenic activity of this compound.

TABLE 1. Plasma lipid and glucose concentrations

Group	Total Cholesterol	Triglyceride	Phosphatidylcholine	Sphingomyelin	Glycosphingolipid	Glucose
			mM		*μM*	*mM*
Group I, baseline (n = 9)	20.9 ± 0.42	0.82 ± 0.05	2.04 ± 0.07	1.26 ± 0.09	16.6 ± 1.5	7.37 ± 0.28
Group II, control (n = 10)	17.8 ± 1.03	0.95 ± 0.05	3.24 ± 0.21	1.44 ± 0.11	20.0 ± 1.4	7.69 ± 0.34
P (group I vs. group II)	0.017	NS	<0.0001	NS	NS	NS
Group III, myriocin (n = 10)	7.64 ± 0.41	0.78 ± 0.04	2.87 ± 0.16	0.66 ± 0.04	15.9 ± 0.7	8.02 ± 0.36
P (group II vs. group III)	<0.0001	0.03	NS	<0.0001	0.014	NS
P (group I vs. group III)	<0.0001	NS	0.0002	0.0003	NS	NS

Apolipoprotein E gene knockout mice were fed a high-fat diet for 30 days. A control group of 10 mice was euthanized at 30 days (group I). Two replicate groups of 10 mice were placed on a regular chow diet for 60 days (group II) or regular chow plus myriocin to yield a dose of 0.3 mg/kg/day for 60 days (group III), and fasted plasma lipids and glucose were determined for all groups as described in Materials and Methods. Data shown are means ± SEM. Significance was assessed by Student's *t*-test.

We also examined the impact of myriocin on the expression of hepatic genes known to regulate lipoprotein metabolism. For this analysis, we focused on apoB, ABCA1, and apoA-I. Hepatic apoA-I mRNA expression was increased significantly (2.6-fold) by myriocin, whereas apoB and ABCA1 mRNA levels were unaltered (**Fig. 5A**). To confirm that the myriocin-induced upregulation of apoA-I gene expression translated to the protein level, liver and plasma apoA-I levels were analyzed by Western blotting. The data indicate that both hepatic and plasma apoA-I concentrations were increased significantly (45% and 38%, respectively) in the myriocin-treated mice (group III) compared with the control group (group II) (Fig. 5B, C). These data suggest that under our experimental conditions, at

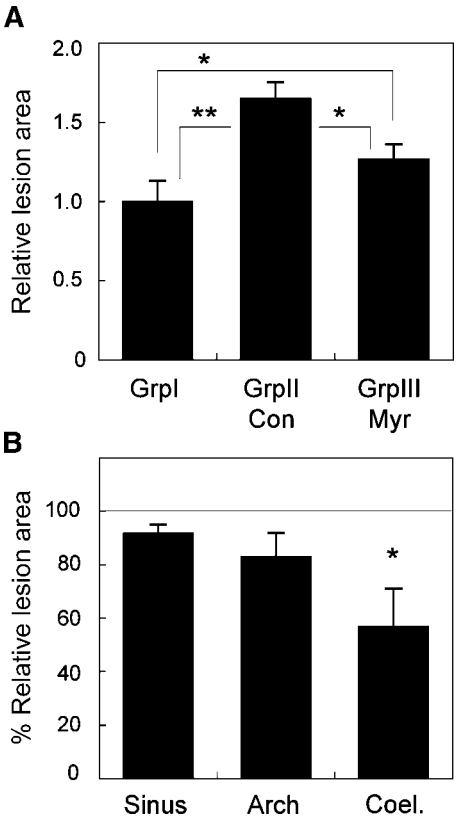

Fig. 3. Morphometric analysis of atherosclerotic lesions. A: ApoE$^{-/-}$ mice were fed a high-fat diet for 30 days. A control group of 10 mice was euthanized at 30 days, and baseline lesion areas for the sinus, arch, and celiac branch point were established and assigned a value of 1.0 (GrpI). Two replicate groups of 10 mice were placed on a regular chow diet for 60 days (GrpII) or regular chow plus myriocin (0–3 mg/kg/day) for 60 days (GrpIII). B: Relative lesion areas were also analyzed site-specifically for groups II and III to determine whether myriocin affects lesion progression uniformly (within the proximal and distal aorta). Group II lesion areas for each site were assigned a value of 100% and are represented by the horizontal line. The SEM values associated with each of the group II 100% values were 4.6, 10.8, and 10.3% for sinus, arch, and celiac, respectively. Data shown are means ± SEM. * $P < 0.05$, ** $P < 0.01$, assessed by Mann-Whitney U test.

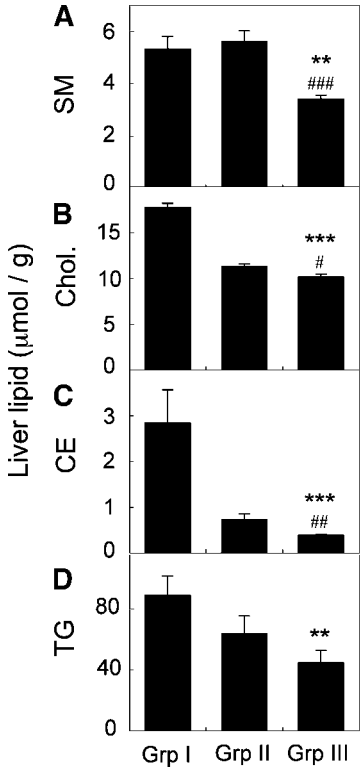

Fig. 4. Liver lipid analysis. ApoE$^{-/-}$ mice were fed a high-fat diet for 30 days (Grp I) and then switched to regular chow (Grp II) or regular chow containing myriocin (0–3 mg/kg/day) (Grp III) for a further 60 days. Hepatic sphingomyelin (SM; A), unesterified cholesterol (Chol.; B), cholesteryl ester (CE; C), and triglyceride (TG; D) contents were analyzed as described in Materials and Methods, and all lipids are expressed as μmol/g liver wet weight. Data shown are means ± SEM. ** $P < 0.01$, *** $P < 0.0001$ (group III vs. group I); $^{\#}$ $P < 0.05$, $^{\#\#}$ $P < 0.01$, $^{\#\#\#}$ $P < 0.0001$ (group III vs. group II), assessed by Student's *t*-test.

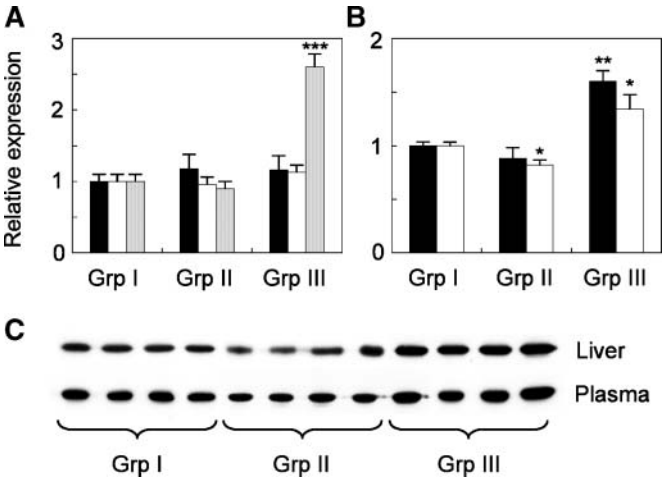

Fig. 5. Analysis of hepatic gene expression and plasma and hepatic apoA-I expression. ApoE$^{-/-}$ mice were fed a high-fat diet for 30 days (Grp I) and then switched to regular chow (Grp II) or regular chow containing myriocin (0–3 mg/kg/day) (Grp III) for a further 60 days. A: Hepatic apoB (black bars), ABCA1 (white bars), and apoA-I (gray bars) mRNA expression was assessed by quantitative real-time PCR, and data are expressed relative to group I values. B, C: Hepatic (black bars) and plasma (white bars) apoA-I protein expression was analyzed by Western blotting, and signal intensity of the apoA-I bands was quantified by ImageJ software. Data are expressed relative to group I values. Data shown are means ± SEM and are derived from a subset of four mice selected at random from each group. * $P < 0.05$, ** $P < 0.01$, *** $P < 0.0001$ (group III or group II vs. group I), assessed by Student's *t*-test.

least part of the antiatherogenic effect of myriocin is related to increased hepatic apoA-I production.

DISCUSSION

Hypercholesterolemia is a major risk factor for atherosclerosis, and it is clear that HMG-CoA reductase inhibitors (statins) effectively decrease serum total cholesterol and LDL-cholesterol and reduce cardiovascular morbidity and mortality (32). However, it is known that a significant number of patients are either resistant to or intolerant of statins, and with recent guidelines for LDL-cholesterol levels to be reduced to <2 mM, it has been reported that <50% of patients treated with statins achieve their targets (33). To address this problem, statin combination therapies are under investigation, for example using the cholesterol absorption inhibitor ezetimibe (33). An underlying tenet of our current work is that, as an adjunct to statin therapy, approaches targeting proatherogenic pathways that are not specifically aimed at reducing cholesterol synthesis or absorption may result in a two-pronged approach to treat atherosclerosis. We and others have proposed that therapeutic targeting of the sphingolipid biosynthetic pathway represents a feasible approach to treat atherosclerosis (see Ref. 22 and references cited therein).

Although myriocin has been shown to inhibit the development of atherosclerosis in apoE$^{-/-}$ mice when it is administered before or concomitant with the onset of lesion formation (23–25, 31), its ability to slow the progression of existing atherosclerosis (or to induce the regression of lesion size) was unknown, and we show here for the first time that whereas lesion progression was inhibited significantly, regression was not induced under the present experimental conditions. We recognize that myriocin treatment may have additional beneficial effects on lesion composition that may not be detected by simply measuring plaque area, such as in macrophage content at the shoulder regions of the lesion cap or collagen composition (23, 31) (both parameters that may affect plaque stability). However, in a preliminary analysis of macrophage and collagen content of lesions, we could not detect a significant change in the myriocin-treated (group III) versus the control (group II) group (E. Glaros, W. Kim, and B. Garner, unpublished data). Interestingly, myriocin inhibited the progression of atherosclerotic lesions effectively only at the distal regions of the aorta. At present, the reasons for this site-specific action are unclear; however, this may be a general phenomenon associated with the pharmacological treatment of apoE$^{-/-}$ mice, since the antiatherogenic actions of other compounds, such as vitamin E plus coenzyme Q_{10} (34) and probucol (35), are also more potent at the distal lesion sites.

Our data indicate that modulation of hepatic and plasma lipid metabolism may contribute to the antiatherogenic action of myriocin. The analysis of plasma lipids highlights the fact that myriocin targets not only SM and GSL synthesis but also decreases cholesterol and TG levels in vivo. The finding that myriocin treatment reduced cholesterol when mice consumed a regular chow diet is noteworthy, as previous data showing that myriocin reduced plasma cholesterol when mice were fed a HF diet (23, 31) have been suggested to be at least partially attributable to direct effects of myriocin on the gastrointestinal absorption of the high levels of cholesterol present in a HF diet (24). Our data indicate that the hypocholesterolemic action of myriocin is in fact not dependent on a high-cholesterol diet. The finding that myriocin significantly increases hepatic and plasma apoA-I levels in the present study is consistent with the suggestion that increased plasma HDL concentration also contributes to the antiatherogenic actions of this compound when animals are fed a HF diet (31).

Although there is increasing evidence that myriocin induces favorable changes in plasma lipid profile, the dominant mechanism(s) by which myriocin inhibits both the development of atherosclerosis (23–25) and the progression of established atherosclerosis (as shown here) is still not entirely clear, as the levels of several classes of potentially atherogenic sphingolipids (including SM, GSLs, and sphingosine-1-phosphate) are affected (22–25). When myriocin is administered orally, reductions in plasma cholesterol may contribute to atherosclerosis inhibition; however, cholesterol reductions are not crucial for antiatherogenic activity, as intraperitoneal administration of myriocin clearly inhibits lesion formation without any significant effect on plasma cholesterol levels. The relative

contributions that myriocin-induced reductions in SM and GSL levels make in the inhibition of atherosclerosis are also not clear, as both the intraperitoneal and oral delivery routes significantly reduce levels of both sphingolipids. The development of more selective compounds to specifically target these sphingolipids will help resolve this issue (22). Potentially relevant to this idea, the GSL synthesis inhibitor *N*-butyl deoxynojirimycin may provide further information in the apoE$^{-/-}$ atherosclerosis model. One potential problem with this compound, however, is that it may also inhibit the *N*-glycan-processing enzymes α-glucosidases I and II and through this action enhance macrophage class A macrophage scavenger receptor expression (which would be predicted to be proatherogenic) (36).

We previously showed that the GSL synthesis inhibitor 1-phenyl-2-decanoylamino-3-morpholino-1-propanol induces ABCA1 transcription and promotes apoA-I-mediated cholesterol efflux from human fibroblasts and macrophages. A major effect of myriocin on ABCA1 transcription seems unlikely in the present in vivo setting, as hepatic ABCA1 mRNA levels were not altered under conditions that reduced SM synthesis by 40%. In preliminary in vitro experiments, we found that apoA-I-mediated cholesterol efflux was stimulated by 30% from human fibroblasts and by 23% from murine macrophages (E. Glaros, W. Kim, and B. Garner, unpublished data); therefore, a subtle effect of myriocin on aspects of the reverse cholesterol transport pathway that remain to be defined cannot be ruled out entirely.

In summary, we have shown that myriocin inhibits the progression of established atherosclerosis in apoE$^{-/-}$ mice and that the antiatherogenic effect is more pronounced in the abdominal aorta than at the sinus and arch. This antiatherogenic activity was associated with significant reductions in the concentrations of plasma cholesterol, TG, SM, and GSL levels and significant increases in plasma and hepatic apoA-I levels. Although previous data indicated that lesion development can be inhibited by up to 93% in apoE$^{-/-}$ mice (using the same dose and administration route we used here) (23), this highly efficacious agent does not appear to promote the regression of established lesions within the time frame we studied. Whether coadministration of myriocin and a statin would stimulate lesion regression in apoE$^{-/-}$ mice remains to be determined.

This work was supported by the National Heart Foundation of Australia and the Australian National Health and Medical Research Council.

REFERENCES

1. Lusis, A. J. 2000. Atherosclerosis. *Nature.* **407:** 233–241.
2. Hansson, G. K. 2005. Inflammation, atherosclerosis, and coronary artery disease. *N. Engl. J. Med.* **352:** 1685–1695.
3. Libby, P., P. M. Ridker, and A. Maseri. 2002. Inflammation and atherosclerosis. *Circulation.* **105:** 1135–1143.
4. SSSS Group. 1994. Randomised trial of cholesterol lowering in 4444 patients with coronary heart disease: the Scandinavian Simvastatin Survival Study (4S). *Lancet.* **344:** 1383–1389.
5. Shepherd, J., S. M. Cobbe, I. Ford, C. G. Isles, A. R. Lorimer, P. W. MacFarlane, J. H. McKillop, and C. J. Packard. 1995. Prevention of coronary heart disease with pravastatin in men with hypercholesterolemia. West of Scotland Coronary Prevention Study Group. *N. Engl. J. Med.* **333:** 1301–1307.
6. Nissen, S. E., S. J. Nicholls, I. Sipahi, P. Libby, J. S. Raichlen, C. M. Ballantyne, J. Davignon, R. Erbel, J. C. Fruchart, J. C. Tardif, et al. 2006. Effect of very high-intensity statin therapy on regression of coronary atherosclerosis: the ASTEROID trial. *J. Am. Med. Assoc.* **295:** 1556–1565.
7. Blumenthal, R. S., and N. K. Kapur. 2006. Can a potent statin actually regress coronary atherosclerosis? *J. Am. Med. Assoc.* **295:** 1583–1584.
8. Smith, E. B. 1960. Intimal and medial lipids in human aortas. *Lancet.* **1:** 799–803.
9. Breckenridge, W. C., J. L. Halloran, K. Kovacs, and M. D. Silver. 1975. Increase of gangliosides in atherosclerotic human aortas. *Lipids.* **10:** 256–259.
10. Prokazova, N. V., and L. D. Bergelson. 1994. Gangliosides and atherosclerosis. *Lipids.* **29:** 1–5.
11. Mukhin, D. N., F. F. Chao, and H. S. Kruth. 1995. Glycosphingolipid accumulation in the aortic wall is another feature of human atherosclerosis. *Arterioscler. Thromb. Vasc. Biol.* **15:** 1607–1615.
12. Jiang, X. C., F. Paultre, T. A. Pearson, R. G. Reed, C. K. Francis, M. Lin, L. Berglund, and A. R. Tall. 2000. Plasma sphingomyelin level as a risk factor for coronary artery disease. *Arterioscler. Thromb. Vasc. Biol.* **20:** 2614–2618.
13. Garner, B., D. A. Priestman, R. Stocker, D. J. Harvey, T. D. Butters, and F. M. Platt. 2002. Increased glycosphingolipid levels in serum and aortae of apolipoprotein E gene knockout mice. *J. Lipid Res.* **43:** 205–214.
14. Guyton, J. R., and K. F. Klemp. 1996. Development of the lipid-rich core in human atherosclerosis. *Arterioscler. Thromb. Vasc. Biol.* **16:** 4–11.
15. Schissel, S. L., J. Tweedie-Hardman, J. H. Rapp, G. Graham, K. J. Williams, and I. Tabas. 1996. Rabbit aorta and human atherosclerotic lesions hydrolyze the sphingomyelin of retained low-density lipoprotein. Proposed role for arterial-wall sphingomyelinase in subendothelial retention and aggregation of atherogenic lipoproteins. *J. Clin. Invest.* **98:** 1455–1464.
16. Garner, B., H. R. Mellor, T. D. Butters, R. A. Dwek, and F. M. Platt. 2002. Modulation of THP-1 macrophage and cholesterol-loaded foam cell apolipoprotein-E levels by glycosphingolipids. *Biochem. Biophys. Res. Commun.* **290:** 1361–1367.
17. Glaros, E. N., W. S. Kim, C. M. Quinn, J. Wong, I. Gelissen, W. Jessup, and B. Garner. 2005. Glycosphingolipid accumulation inhibits cholesterol efflux via the ABCA1/apoA-I pathway. 1-Phenyl-2-decanoylamino-3-morpholino-1-propanol is a novel cholesterol efflux accelerator. *J. Biol. Chem.* **280:** 24515–24523.
18. Gong, N., H. Wei, S. H. Chowdhury, and S. Chatterjee. 2004. Lactosylceramide recruits PKCalpha/epsilon and phospholipase A2 to stimulate PECAM-1 expression in human monocytes and adhesion to endothelial cells. *Proc. Natl. Acad. Sci. USA.* **101:** 6490–6495.
19. Bhunia, A. K., H. Han, A. Snowden, and S. Chatterjee. 1997. Redox-regulated signaling by lactosylceramide in the proliferation of human aortic smooth muscle cells. *J. Biol. Chem.* **272:** 15642–15649.
20. Prokazova, N. V., I. A. Mikhailenko, and L. D. Bergelson. 1991. Ganglioside GM3 stimulates the uptake and processing of low density lipoproteins by macrophages. *Biochem. Biophys. Res. Commun.* **177:** 582–587.
21. Levade, T., N. Auge, R. J. Veldman, O. Cuvillier, A. Negre-Salvayre, and R. Salvayre. 2001. Sphingolipid mediators in cardiovascular cell biology and pathology. *Circ. Res.* **89:** 957–968.
22. Kim, W. S., C. E. Chalfant, and B. Garner. 2006. Fine tuning therapeutic targeting of the sphingolipid biosynthetic pathway to treat atherosclerosis. *Curr. Vasc. Pharmacol.* **4:** 151–154.
23. Park, T. S., R. L. Panek, S. B. Mueller, J. C. Hanselman, W. S. Rosebury, A. W. Robertson, E. K. Kindt, R. Homan, S. K. Karathanasis, and M. D. Rekhter. 2004. Inhibition of sphingomyelin synthesis reduces atherogenesis in apolipoprotein E-knockout mice. *Circulation.* **110:** 3465–3471.
24. Hojjati, M. R., Z. Li, H. Zhou, S. Tang, C. Huan, E. Ooi, S. Lu, and X. C. Jiang. 2005. Effect of myriocin on plasma sphingolipid metabolism and atherosclerosis in apoE-deficient mice. *J. Biol. Chem.* **280:** 10284–10289.
25. Glaros, E. N., W. S. Kim, B. J. Wu, C. Suarna, C. M. Quinn, K. A. Rye, R. Stocker, W. Jessup, and B. Garner. 2007. Inhibition of ath-

erosclerosis by the serine palmitoyl transferase inhibitor myriocin is associated with reduced plasma glycosphingolipid concentration. *Biochem. Pharmacol.* **73:** 1340–1346.
26. Hojjati, M. R., and X. C. Jiang. 2006. Rapid, specific, and sensitive measurements of plasma sphingomyelin and phosphatidylcholine. *J. Lipid Res.* **47:** 673–676.
27. Garner, B., A. Baoutina, R. T. Dean, and W. Jessup. 1997. Regulation of serum-induced lipid accumulation in human monocyte-derived macrophages by interferon-gamma. Correlations with apolipoprotein E production, lipoprotein lipase activity and LDL receptor-related protein expression. *Atherosclerosis.* **128:** 47–58.
28. Turunen, M., and S. Schedin-Weiss. 2007. Defect in fatty acid esterification of dolichol in Niemann-Pick type C1 mouse livers in vivo. *Biochim. Biophys. Acta.* **1771:** 506–513.
29. Plump, A. S., J. D. Smith, T. Hayek, K. Aalto-Setala, A. Walsh, J. G. Verstuyft, E. M. Rubin, and J. L. Breslow. 1992. Severe hypercholesterolemia and atherosclerosis in apolipoprotein E-deficient mice created by homologous recombination in ES cells. *Cell.* **71:** 343–353.
30. Nakashima, Y., A. S. Plump, E. W. Raines, J. L. Breslow, and R. Ross. 1994. ApoE-deficient mice develop lesions of all phases of atherosclerosis throughout the arterial tree. *Arterioscler. Thromb.* **14:** 133–140.
31. Park, T. S., R. L. Panek, M. D. Rekhter, S. B. Mueller, W. S. Rosebury, A. Robertson, J. C. Hanselman, E. Kindt, R. Homan, and S. K. Karathanasis. 2006. Modulation of lipoprotein metabolism by inhibition of sphingomyelin synthesis in apoE knockout mice. *Atherosclerosis.* **189:** 264–272.
32. Ballantyne, C. M., J. A. Herd, J. K. Dunn, P. H. Jones, J. A. Farmer, and A. M. Gotto, Jr. 1997. Effects of lipid lowering therapy on progression of coronary and carotid artery disease. *Curr. Opin. Lipidol.* **8:** 354–361.
33. Ballantyne, C. M. 2005. Rationale for targeting multiple lipid pathways for optimal cardiovascular risk reduction. *Am. J. Cardiol.* **96:** 14K–19K.
34. Thomas, S. R., S. B. Leichtweis, K. Pettersson, K. D. Croft, T. A. Mori, A. J. Brown, and R. Stocker. 2001. Dietary cosupplementation with vitamin E and coenzyme Q(10) inhibits atherosclerosis in apolipoprotein E gene knockout mice. *Arterioscler. Thromb. Vasc. Biol.* **21:** 585–593.
35. Witting, P. K., K. Pettersson, J. Letters, and R. Stocker. 2000. Site-specific antiatherogenic effect of probucol in apolipoprotein E-deficient mice. *Arterioscler. Thromb. Vasc. Biol.* **20:** E26–E33.
36. Tian, G., D. Wilcockson, V. H. Perry, P. M. Rudd, R. A. Dwek, F. M. Platt, and N. Platt. 2004. Inhibition of alpha-glucosidases I and II increases the cell surface expression of functional class A macrophage scavenger receptor (SR-A) by extending its half-life. *J. Biol. Chem.* **279:** 39303–39309.